Reactions of nitrogen and oxygen surface groups in nanoporous carbons under inert and reducing atmospheres — Source link 🔗

Bo Xiao, J. P. Boudou, K.M. Thomas

Institutions: Newcastle University

Topics: Thermal desorption spectroscopy, Adsorption, Thermal desorption, Desorption and Functional group

Related papers:

- Evolution of nitrogen functionalities in carbonaceous materials during pyrolysis

- Modification of the surface chemistry of activated carbons

- Determination of the Fate of Nitrogen Functionality in Carbonaceous Materials during Pyrolysis and Combustion Using X-ray Absorption Near Edge Structure Spectroscopy

- Nitrogen-doped carbon nanotube arrays with high electrocatalytic activity for oxygen reduction.

- Quantification of nitrogen forms in Argonne Premium coals

Reactions of Nitrogen and Oxygen Surface Groups in Nanoporous Carbons under Inert and Reducing Atmospheres

B. Xiao, Jean-Paul Boudou, Mark Thomas

Reactions of Nitrogen and Oxygen Surface Groups in Nanoporous Carbons under Inert and Reducing Atmospheres

B. Xiao, J. P. Boudou, and K. M. Thomas*

Northern Carbon Research Laboratories, School of Natural Sciences, Bedson Building, University of Newcastle upon Tyne, Newcastle upon Tyne, NE1 7RU United Kingdom, and University Pierre et Marie Curie, CNRS 4, Place Jussieu, 75252 Paris Cedex 05, France

The reactions of surface functional groups have an important role in controlling conversion of char nitrogen to NOx during coal combustion. This study involved an investigation of the thermal stability and reactions of nitrogen surface functional groups in nanoporous carbons. Four suites of carbons, which were used as models for coal chars, were prepared with a wide range of nitrogen and oxygen contents and types of functional groups. The porous structures of the carbons were characterized by gas adsorption methods while chemical analysis, X-ray photoelectron spectroscopy, and X-ray near edge structure spectroscopy were used to characterize the surface functional groups. Temperature programmed desorption and temperature programmed reduction methods were used to study the reactivity of the surface functional groups during heat treatment under inert and reducing conditions. Heat treatment studies show that the order of stability of the functional groups is quaternary nitrogen > pyridinic > pyrrolic > pyridine *N*-oxide. Pyridine *N*-oxide surface groups desorb NO and form N_2 via surface reactions at low temperature. Pyrrolic and pyridinic functional groups decompose and react with surface species to give NH_3, HCN, and N_2 as desorption products, but most pyrrolic groups are preferentially converted to pyridinic and quaternary nitrogen. The main desorption product is N_2. Approximately 15–40 wt % of the original nitrogen was retained in the carbons mainly as quaternary nitrogen after heat treatment to 1673 K. The results are discussed in terms of decomposition ranges for surface functional groups and reaction mechanisms of surface species.

1. Introduction

The environmental impact of coal combustion for power generation is a major concern.[1] Technologies have been developed to make coal combustion more environmentally acceptable, including improvements in combustion efficiencies, flue gas desulfurization, and the development of combustion technologies for minimizing NOx emissions. In the case of the latter, this often involves the use of lower combustion temperatures to reduce emissions due to the Zeldovich mechanism and devolatilization of the coal in a low oxygen concentration environment. This leads to problems with carbon burn-out leading to lower efficiency, and nitrogen bound in the carbon char structure after devolatilization becomes the major source of NOx.[1,2]

Nitrogen is present in the organic structure of coal, in the form of pyridinic, pyrrolic, and quaternary functionalities,[3-9] and a large amount is retained in the char after the devolatilization process. The forms of nitrogen in coal chars[10,11] and chars derived from nitrogen-containing pure organic compounds and polymers [12-14] have been studied by X-ray photoelectron spectroscopy (XPS) and X-ray absorption near edge structure (XANES) spectroscopy[14,15] and are pyridinic, pyrrolic, pyridone, pyridine *N*-oxide, amine, and quaternary nitrogen.[12-14]

NOx release during coal combustion is related to the following mechanisms: (i) evolution of nitrogen content and functionality during pyrolysis and combustion, (ii) release of char nitrogen species to the gas phase and its further oxidation, and (iii) rate of NO reaction with the char.[1] NO is the primary product of char nitrogen combustion. The other nitrogen products of carbon char combustion, N_2 and N_2O, are thought to the result from either secondary homogeneous or heterogeneous surface reactions. Nitrogen functionalities may react or decompose during pyrolysis and there is evidence for the formation of pyridone and pyridine *N*-oxide functional groups during combustion and gasification. [14,16] All these factors influence the relative rates of various reactions and, therefore, product distributions and are critical in determining the conversion of char nitrogen to NO. [1,2]

* To whom all correspondence should be addressed. E-mail: mark.thomas@ncl.ac.uk.

(1) Molina, A.; Eddings, E. G.; Pershing, D. W.; Sarofim, A. F. *Prog. Energy Combust. Sci.* **2000,** *26,* 507.

(2) Harding, A. W.; Brown, S. D.; Thomas, K. M. *Combust. Flame* **1996,** *107 (4),* 336.

(3) Thomas, K. M. *Fuel* **1997,** *76,* 457.

(4) Boudou, J. P.; Mariotti, A.; Oudin, J. L. *Fuel* **1984,** *63,* 1508.

(5) Burchill, P.; Welch, L. S. *Fuel* **1989,** *68,* 100.

(6) Mullins, O. C.; Mitra-Kirtley, S.; van Elp, J.; Cramer, S. P. *Appl. Spectrosc.* **1993,** *47,* 1268.

(7) Wallace, S.; Bartle, K. D.; Perry, D. L. *Fuel* **1989,** *68,* 1450.

(8) Kelly, M. D.; Buckley, A. N.; Nelson, P. F. *Proceedings of the International Conference on Coal Science,* University of Newcastle-Upon-Tyne, UK, Sept 16-20, 1991; Butterworth-Heinemann: Oxford, 1991; p 356.

(9) Wojtowicz, M. A.; Pels, J. R.; Moulijn, J. A. *Fuel* **1994,** *73,* 1416.

(11) Gong, B.; Buckley, A. N.; Lamb, R. N.; Nelson, P. F. *Surf. Interface Anal.* **1999,** *28 (1),* 126.

(12) Kelemen, S. R.; Gorbaty, M. L.; Kwiatek, P. J.; Fletcher, T. H.; Watt, M.; Solum, M. S.; Pugmire, R. J. *Energy Fuels* **1998,** *12 (1),* 159.

(13) Pels, J. R.; Kapteijn, F.; Moulijn, J. A.; Zhu, Q.; Thomas, K. M. *Carbon* **1995,** *33,* 1641.

(14) Stanczyk, K.; Dziembaj, R.; Piwowarska, Z.; Witkowski, S. *Carbon* **1995,** *33,* 1383.

(15) Zhu, Q.; Money, S. L.; Russell, A. E.; Thomas, K. M. *Langmuir* **1997,** *13,* 2149.

(16) Jones, J. M.; Zhu, Q.; Thomas, K. M. *Carbon* **1999,** *37,* 1123.

(17) Kapteijn, F.; Moulijn, J. A.; Matzner, S.; Boehm, H.-P. *Carbon* **1999,** *37 (7),* 1143.

The release of char nitrogen during combustion involves reactions on the surface and in the pores of the carbon, and nitrogen is retained in the char.[3,17] The NO-carbon reaction is important,[18-26] and oxygen enhances the NO-carbon reaction while decreasing the nitrous oxide carbon reaction. This is thought to be related to the different modes of adsorption of NO and N_2O.[18] N_2 is the major product of the carbon-NO reaction, and the mechanism of this reaction has been studied in some detail. Interestingly, NO has been shown to form cyano functionalities on carbon surfaces which can form HCN during combustion.[26] Small amounts of reactive intermediate species, HCN and C_2N_2, indicative of surface reactions, were evolved during temperature programmed combustion.[27] The complexity of the process has led to applications of *ab initio* molecular orbital calculations and density functional theory to understand the surface chemistry of desorption of surface species and reactions of nitrogen oxides in the presence of surface oxygen species on the surface of carbon, to understand the reduction of NO during char combustion.[28-34] Density functional theory has been used to study the reaction of NO with char-bound nitrogen and the role of preadsorbed oxygen.[17] The calculations indicate that the presence of adsorbed oxygen on the carbon basal plane containing nitrogen enhances the reduction of NO to N_2.

In this study, the thermal evolution and reactions of nitrogen surface species under inert and reducing conditions and desorption of nitrogen species were investigated in four suites of carbons. These carbons were used as models for coal chars to avoid possible catalytic effects due to the presence of inorganic materials. Inert and hydrogen-rich conditions are relevant to the char devolatilization stage. Reactions of nitrogen, oxygen, and hydrogen surface groups were investigated using temperature programmed desorption (TPD) and temperature programmed reduction (TPR). The results are discussed in relation to surface groups identified by XANES and XPS to gain an improved insight into the role of specific functional groups in surface reactions involved in the release of nitrogen-containing species during char pyrolysis, gasification, and combustion.

(17) Ashman, P. J.; Haynes, B. S.; Buckley, A. N.; Nelson, P. F. *Symp. (Int.) Combust., [Proc.], 27th* **1998,** *2,* 3069.
(18) Yamashita, H.; Tomita, A.; Yamada, H.; Kyotani, T.; Radovic, L. R. *Energy Fuels* **1993,** *7,* 85.
(19) Aarna, I.; Suuberg, E. M. *Symp. (Int.) Combust., [Proc.], 27th* **1998,** *2,* 3061.
(20) Aarna, I.; Suuberg, E. M. *Fuel* **1997,** *76,* 475.
(21) Chan, L. K.; Sarofim, A. F.; Beer, J. M. *Combust. Flame* **1983,** *52 (1),* 37.
(22) Chambrion, P.; Orikasa, H.; Suzuki, T.; Kyotani, T.; Tomita, A. *Fuel* **1997,** *76,* 493.
(23) Furusawa, T.; Tsunada, M.; Tsujimura, M.; Adschiri, T. *Fuel* **1985,** *64,* 1306.
(24) Yang, J.; Mestl, G.; Herein, D.; Schlogl, R.; Find, J. *Carbon* **2000,** *38,* 715; *Carbon* **2000,** *38,* 729.
(25) Aarna, I.; Suuberg, E. M. *Energy Fuels* **1999,** *13,* 1145.
(26) Chambrion, P.; Kyotani, T.; Tomita, A. *Symp. (Int.) Combust., [Proc.] 27th* **1998,** *2, 3053.*
(27) Jones, J. M.; Harding, A. W.; Brown, S. D.; Thomas, K. M. *Carbon* **1995,** *33,* 833.
(28) Kyotani, T.; Tomita, A. *J. Phys. Chem. B* **1999,** *103,* 3434.
(29) Montoya, A.; Truong, T. N.; Sarofim, A. F. *J. Phys. Chem. A* **2000,** *104,* 8409.
(30) Zhu, Z. H.; Finnerty, J.; Lu, G. Q.; Yang, R. T. *J. Phys. Chem. B* **2001,** *105,* 821.
(31) Montoya, A.; Truong, T. T.; Mondragon, F.; Truong, T. N. *J. Phys. Chem. A* **2001,** *105,* 6757.
(32) Wongtanakitcharoen, S.; Tatiyakiatisakun, T.; Rirksomboon, T.; Long, R. Q.; Osuwan, S.; Malakul, P.; Yang, R. T. *Energy Fuels* **2001,** *15,* 1341.
(33) Byrne, C. P.; Yang, R. T.; Zhu, Z. H.; Lu, G. Q. *J. Phys. Chem. B* **2002,** *106,* 2592.
(34) Zhu, Z. H.; Lu, G. Q. *Energy Fuels* **2003,** *17,* 1057.

2. Experimental Section

2.1. Precursor Materials Used. *Carbon Material Used.* Commercially available coconut shell derived carbon G prepared by physical activation using steam at 1173 K was used in this study. This carbon was supplied by Pica, Vierzon, France.

Polyacrylonitrile (PAN) Derived Carbon. PAN powder supplied by Aldrich Chemical Co. was pretreated in air at 473 K for 1 h. The pretreated PAN was heated at a rate of 3 K min^{-1} to 1173 K in argon. The argon flow was then changed to CO_2, and the char was gasified at 1173 K for 4h. This gave a carbon, designated code PANC, which had a burnoff — 60 wt %.

Acridine Carbon. Acridine (99% pure) was obtained from Aldrich Chemical Co. Acridine was carbonized under argon at a pressure of 4.1 MPa with a heating rate of 1 K min^{-1} to a final temperature of 873 K and held at the heat treatment temperature (HTT) for 1 h to give carbon AD873. The sample produced by high-pressure carbonization was then heat treated at atmospheric pressure to 1073 K at a heating rate of 4 K min^{-1} under argon and held at the HTT for 1 h to give carbon AD1073.

2.2. Treatment Procedures. PANC and G were subjected to low temperature chemical oxidation followed by heat treatment to systematically vary the type and concentration of oxygen functional groups. This gave two series of carbons with (a) low nitrogen contents (^-1 wt %) derived from G and (b) a high nitrogen content (^8 wt %) series derived from PANC. Carbons G and chemically oxidized G (GN) were treated with ammonia. It was envisaged that different types of functional groups might be incorporated by high-temperature gasification compared with nitrogen incorporation during the carbonization procedure. This gave a third series of carbons with a range nitrogen contents. A fourth series of carbons was prepared by carbonization of a starting material with well-defined pyridinic nitrogen functionality (acridine). Both the ammonia treated and acridine carbon samples were partially combusted at 1073 K to incorporate carbonyl groups for comparison with the low-temperature chemical oxidation method.[35] The four series of carbons (see Table 1) had a wide range of nitrogen and oxygen contents and, also, very low ash contents (see Table 2).

Chemical Oxidation Treatment. G and PANC were refluxed in a 7.5 M HNO_3 solution for 48 h. The oxidized carbons were Soxhlet extracted with water, to remove residual HNO_3 and any soluble materials, until the pH of the aqueous extract was constant, and vacuum-dried at 348 K. The carbons derived from PANC and G were designated sample codes PANCN and GN, respectively.

Ammonia Treatment. G and GN were heated to 1073 K at a heating rate of 3 K min^{-1} in ammonia (flow rate ^- 200 cm^3 min^{-1}) and held at the maximum temperature for 3 h. The treated carbon was cooled in ammonia to room temperature. The carbon was then Soxhlet extracted with water to remove residual ammonia and any soluble material. The sample was vacuum-dried at 348 K. The carbons derived from G and GN were designated sample codes GA and GNA, respectively.

Heat Treatment Procedures. PANCN and GN were heat treated to provide a suite of carbons where the oxygen functional groups of various thermal stabilities were varied progressively. The carbon samples were heat treated to the HTT at 3 K min^{-1} and held at the HTT for 1 h. The resultant carbons were designated using the code of original carbon and the HTT in kelvin; for example, GN573 represents GN heat treated to 573 K and held at the HTT for 1 h.
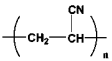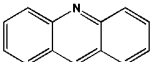
Partial Combustion Treatment. GNA, GA, and AD1073 were partially gasified in 20% oxygen/argon until the specified extent of burnoff. The samples were then cooled in argon to room temperature. The carbons were given sample codes designated by the extent of burnoff; for example, AD1073 with a burnoff of 56% was given the code AD1073-B56.

2.3. Chemical Analyses. Proximate analyses were performed by the method described previously.[36] Elemental analyses were determined by Microanalytical Services, Oakhampton, U.K.

(36) Figueiredo, J. L.; Pereira, M. F. R.; Freitas, M. M. A.; Orfao, J. J. M. *Carbon* **1999,** *37,* 1379,
(37) Grant, K. A.; Zhu, Q.; Thomas, K. M. *Carbon* **1994,** *32,* 883.

Table 1. Methods of Preparation of the Carbon Samples

Carbon samples	Preparation method
PAN carbon series	
Original and Oxidized /Heat Treated Series	$-(CH_2-CH)_n-$ with CN group
PANC	PAN carbonization at 1073 K
PANCN	PANC oxidation with HNO_3
PANCN573	PANCN carbonization at 573 K
PANCN673	PANCN carbonization at 673 K
PANCN873	PANCN carbonization at 873 K
TPD carbon residues	
PANCR	
PANCNR	PANC series carbons after
PANCN573R	programmed desorption up to 1673 K,
PANCN673R	Hold time 0 s
PANCN873R	
Acridine carbon series	(acridine structure)
AD873	Acridine carbonization at 873 K
AD1073	Acridine carbonization at 1073 K
AD1073-B56	AD1073 combustion to56% burn-off
TPD Carbon residues	
AD1073R	Carbon AD1073 after programmed desorption up to 1673 K, Hold time 0 s
Coconut shell G carbon series	
Original G and Oxidized /Heat Treated Series	
G	Coconut shell based activated carbon
GN	G oxidized with HNO_3
GN673	GN carbonized at 673 K
Ammonia Treated G Series	
GA	G or GN treated with NH_3 at 1073 K
GNA	
GNA-B56	GNA combustion with 56% burn-off
TPD carbon residues	
GR	
GNR	G series carbons after programmed desorption up to 1673 K, Hold time 0 s
GAR	
GNAR	

Table 2. Proximate and Elemental Analyses for the Carbons Used in This Study[a]

carbon samples	proximate analysis V_b	A_c	elemental analyses, wt % daf C	H	N	O	atomic ratio ×100 N/C	H/C	O/C
G Carbon series									
G	4.46	2.73	96.22	0.42	0.28	2.95	0.25	5.24	2.29
GN	33.77	0.49	76.34	0.89	1.05	22.36	1.18	13.99	21.97
GN673	19.68	0.92	83.94	0.63	1.05	13.65	1.07	9.01	12.2
PAN Carbon series									
PANC	1.03	0.7	89.28	0.37	8.19	2.18	7.86	4.97	1.83
PANCN	26.64	0.45	72.66	0.99	7.55	19.75	8.91	16.39	20.37
PANCN573	18.72	0.35	75.55	0.85	7.94	14.22	9.01	13.50	14.12
PANCN673	16.28	0.42	77.07	0.95	8.16	13.40	9.08	14.79	13.04
PANCN873	10.27	0.32	82.33	0.93	8.7	7.99	9.06	13.56	7.28
Ammonia Treated Carbons									
GA	2.65	2.48	95.50	0.10	2.30	2.00	2.06	1.26	1.57
GNA	7.19	2.93	90.00	0.50	5.30	3.90	5.05	6.67	3.25
GNA-B56			88.86	0.84	4.77	3.53	4.60	11.25	2.98
Acridine Carbons									
AD1073			89.22	0.86	7.22	1.61	6.94	11.49	1.35
AD1073-B56			88.48	0.94	7.52	2.78	7.29	12.66	2.36
AD873			88.42	2.53	7.53	1.99	7.30	34.1	1.69
Carbons after Heat Treatment to 1673 K, Hold Time 0 s									
PAN Series Carbons									
PANCR			97.38	0.13	2.29		2.02	1.60	
PANCNR			97.83	0.17	2.21		1.94	2.09	
PANCN573R			98.69	0.16	2.39		2.08	1.95	
PANCN673R			97.00	0.15	2.33		2.06	1.86	
PANCN873R			97.16	0.16	2.23		1.97	1.98	
AD1073R			96.55	0.05	3.22		2.86	0.62	
GNR			97.29	0.13	0.35		0.31	1.61	
GNAR			97.41	0.18	0.75		0.66	2.23	
Surface Composition Given by XPS[d]									
GR			96.29	-	0.12	3.59	0.12		3.73
GNR			97.29	-	0.24	2.47	0.25		2.54
GAR			96.73	-	0.15	3.11	0.16		3.22
PANCR			92.34	-	1.21	6.45	1.31		6.99
PANCNR			95.13	-	1.12	3.75	1.18		3.94
AD1073R			96.48	-	1.30	2.22	1.35		2.30

[a] Carbons GA, GNA, and AD were all treated to 1073 K, and, therefore, the volatile matter contents were negligible and were not determined. [b] Volatile content, wt % daf. [c] Ash content, wt % db (dry basis). [d] wt % daf.

2.4. Porous Structure Characterization. The micropore and total pore volumes of active carbons used were evaluated by the adsorption of CO_2 at 273 K and N_2 at 77 K, respectively. The measurements were carried out using a Hiden Analytical, Ltd., intelligent gravimetric analyzer. The micropore volume was obtained from the CO_2 adsorption data $(p/p^0, 0-0.03)$ by extrapolation of the Dubinin–Radushkevich equation[37] to p/p^0) 1. An adsorbed phase density (ρ_{CO2}) of 1.023 cm^3 g^{-1} was used in the calculation. The total pore volume was obtained from the uptake of N_2 at p/p^0) 1 $(\rho_{N2}$ 0.8081 cm^3 $g^{-1})$.

2.5. Functional Group Characterization. *XANES.* Nitrogen K-edge measurements were performed at the Laboratoire pour l'Utilisation du Rayonnement Electromagne´tique (LURE, Orsay, France) on the VUV Super-Aco storage ring. They were carried out at room temperature and 10^{-10} Torr on the Sacemor experiment connected to the SA72 beam line, equipped with a high-energy TGM monochromator (resolution of ^-0.2 eV at the nitrogen K edge). The spectra were recorded with total-electron-yield detection, normalized from the fluctuations in the X-ray intensity by dividing the signal by that of a copper grid freshly

(37) Dubinin, M. M. In *Characterization of Porous Solids;* Sing, K. S. W., Ed.; Society of Chemical Industries: London, 1979; Vol. 1, pp 1-11.

coated with gold, with normal X-ray incidence *(E* parallel to the surface). The samples were dispersed in acetone and applied to high-purity tungsten plates, and the solvent was allowed to evaporate. The nitrogen 1s $_\pi$ peak of CN in PAN at 401.4 eV was used to calibrate the monochromator at the nitrogen K edge.

XPS. A VG Scientific ESCALAB 250 system equipped with a micro-focused, monochromated Al K_R X-ray source (1486.6 eV, 650 -µm spot size, 200 W) and a magnetic immersion lens, which focuses electrons emitted from the sample over a cone of up to (45° into the main lens column of the equipment, were used. The spectra were acquired in constant analyzer energy mode, with pass energies of 150 and 20 eV for the survey and the narrow regions, respectively. The samples were mounted onto conducting double-sided adhesive tape. They did not exhibit any charging effects, and the charge compensation system (a combination of an electron and argon flood guns) was not used.

Advantage software, version 1.85, was used for digital acquisition and data processing. The surface compositions (in atomic %) were determined using the integrated peak areas of C(1s), N(1s), and O(1s) and the respective sensitivity factors. The concentration (%) of a particular element A was computed using

$$\% A \ ) \ \frac{I_A/s_A}{\sum (I_n/s_n)} \times 100\%$$

where I_n and s_n are the integrated peak areas and the sensitivity factors, respectively.

Table 3. Pore Structure Characterization Data for the Active Carbons Used in This Study Determined by Adsorption of Carbon Dioxide at 273 K and Nitrogen at 77 K[a]

carbon samples	pore volume (cm³ g⁻¹)		V_{CO_2}/V_{N2}	$S_{max,c}$ (m² g⁻¹)	$E_{0,e}$ (kJ mol⁻¹)	X_f (nm)
	$V_{CO_2,b}$ (CO₂ at 273 K)	$V_{N,x}$ (N₂ at 77 K)				
G	0.334	0.484	0.690	898	27.14	0.42
GN	0.262	0.366	0.716	704	24.96	0.47
GN673	0.235	0.443	0.530	631	24.23	0.49
PAN	0.153	0.204	0.750	411	33.22	0.29
PANCN	0.112	0.181	0.619	301	32.57	0.31
PANCN573	0.141	0.213	0.662	379	29.55	0.37
PANCN673	0.127	0.216	0.588	341	35.43	0.25
PANCN873	0.148	0.236	0.627	397	32.27	0.31
GA	0.260	0.300	0.866	691		
GNA	0.200	0.300	0.666	529		

Density of the adsorbed phase (g cm⁻³): nitrogen, 0.8081; carbon dioxide, 1.023. Obtained from an intercept of DR plot. Obtained from the Langmuir model at $p/p^0 = 1$. Maximum DR surface area (CO₂ at 273 K, CO₂ cross-sectional area 1.156×10^5 m² mol⁻¹). Characteristic energy in the DR equation (CO₂ at 273 K, 0.35). X is the mean radius of microporosity from Dubinin-Stoeckli method[38] of CO₂ adsorption data at 273 K.

2.6. X-ray Diffraction (XRD). The samples were placed inside Lindemanglass capillaries (0.5-mm diameter). The XRD patterns were recorded using an INEL CPS 120 diffractometer with a cylindrical position-sensitive detector (transmission mode, Debye–Scherer geometry) and Co K$_{R1}$ $_{(A)}$ 1.7889 Å) radiation, from 1 to 120° (2$_0$).

2.7. TPD and TPR. Samples (^-5 mg, particle size $< 80 \mu$m) were heated at 30 K min⁻¹ at atmospheric pressure in a flow (10 cm³ min⁻¹) of a mixture of helium and neon (99:1, v/v). Evolved gases were monitored with a Leybold quadrupole mass spectrometer. N₂ was detected after selective oxidation of CO as CO₂ on MnO₂ at 393 K. Calibration was carried out using Air Liquide standard gas mixtures of the gas in pure helium with 1% neon. The compositions of some of the carbon residues from the TPD experiments were analyzed. These samples are designated with the suffix R; that is, PANCNR represents the residue from the TPD experiment for PANCN.

3. Results and Discussion

3.1. Structural and Analytical Characterization.

3.1.1. Proximate and Elemental Analyses. Proximate and elemental analyses of the carbons used in this study and some of the TPD carbon residues are given in Table 2. The oxygen contents of the low nitrogen content [< 1.05 wt % dry ash free (daf)] carbons G, GN, and GN673 were in the range ^-3–22 wt % daf while the oxygen contents of the high (7–8 wt % daf) nitrogen content PAN series varied in the range ^-2–20 wt % daf oxygen. Heat treatment had a marked affect on the oxygen content but little or no effect on the nitrogen content of the carbons. Carbons with intermediate nitrogen contents were obtained by treating G and GN with ammonia at 1073 K to give carbons GA and GNA, respectively. AD1073 had a high nitrogen content (^-7.2 wt % daf) and was used as the reference carbon.

Analyses of the TPD carbon residues (HTT 1673 K) showed that 15–40% of the original amounts of nitrogen were retained in the PAN series of carbons, AD1073, and GNA while the oxygen and hydrogen contents were negligible (<0.2 wt %).

3.1.2. Porous Structure Characterization Data. The porous structures of the carbon materials were characterized using nitrogen adsorption at 77 K and CO₂ adsorption at 273 K, and the results are given in Table 3. The total
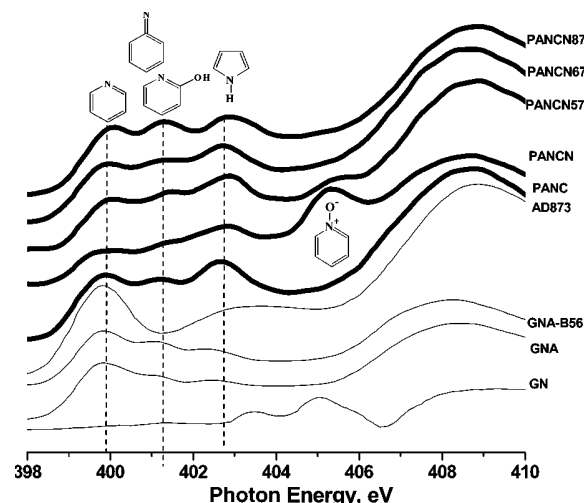

Figure 1. Nitrogen K-edge XANES spectra of PAN, the oxidized/heat treated PAN series, oxidized G(GN), ammonia treated GN(GNA), partially combusted ammonia treated GN-(GNA-B56) and acridine carbons.

pore volumes obtained from nitrogen adsorption and the micropore volumes obtained from CO₂ adsorption do not change greatly with heat treatment within a given series. Therefore, the reactions of surface functional groups in a given series can be studied without marked effects due to changes in porous structure. However, the total pore and micropore volumes of the PANC carbon series are typically 40–60% of the values in the G series of carbons. Table 3 shows the characteristic energies and mean pore radii obtained by the method of Dubinin and Stoeckli.[38] The PAN carbon series have narrower average pore radii than the G series.

3.1.3. XANES Measurements. Nitrogen functional groups were characterized using XANES because of the improved spectral resolution compared with that of XPS. Curve resolution is normally required to resolve the components in XPS, and this leads to uncertainty in the quantification of the peaks. XANES allowed clearer identification of pyridinic, pyridone, and pyrrolic groups. However, XPS studies showed that quaternary nitrogen and oxidized species (N–X) were the major surface nitrogen groups present in carbon TPD residues. The XANES spectra of these surface species have broad bands that are difficult to identify by this technique, whereas XPS allows a clear identification. Therefore, XANES was used to characterize the nitrogen species in carbons with HTT < 1273 K and XPS was used to characterize the TPD residues (HTT of 1673 K)

G Carbon Series. The XANES K-edge spectrum of GN is shown in Figure 1. It is apparent that the main peak at ^-405 eV has a much higher intensity than the other nitrogen peaks at ^-400, 401.5, and 403.5 eV. This peak at 405 eV is due to species incorporated by the nitric acid oxidation procedure. Comparison with reference compounds indicates that the peak is due to pyridine *N*-oxide species. [14] The other peaks are assigned to pyridinic, pyridone, and pyrrolic groups. Pyridine *N*-oxide surface groups were not observed for other carbons where nitrogen is incorporated during the carbonization process.

PAN Carbon Series. The XANES spectra of the PAN series of carbons are shown in Figure 1. The spectrum of PAN has a sharp peak at ^-401.4 eV whereas carbon PANC has broader peaks at 399.8, ^-401, and ^-403 eV. These

(38) Dubinin, M. M.; Stoeckli, H. F. *J. Colloid Interface Sci.* **1980**, *75*, 34.
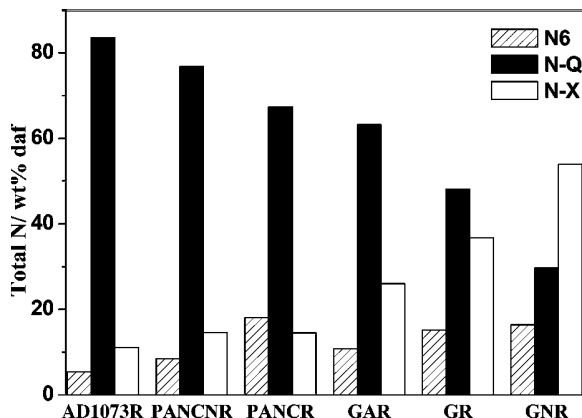
Figure 2. Nitrogen functional group compositions of the TPD carbon residues (HTT 1673 K).

Table 4. XRD Parameters Obtained for TPD Carbon Residue Samples

	observed curve			Pearson VII amplitude fitting		
	position ($°2\theta$)	fwhm ($°2\theta$)	L_c (Å)	position ($°2\theta$)	fwhm ($°2\theta$)	L_c (Å)
AD1073R	30.34	3.20	29.55	30.15	3.15	29.98
PANCR	29.67	5.10	18.51	29.27	5.18	18.21
PANCNR	29.38	6.90	13.67	29.07	7.01	13.45
GR	27.96	5.80	16.22	28.60	6.02	15.65
GNR	29.35	5.10	18.50	29.12	4.67	20.17
GAR	29.35	4.50	20.96	29.21	4.63	20.37

bands are consistent with the presence of pyridinic, pyridone (or cyanide), and pyrrolic functional groups. PANCN has peaks due to pyridinic, pyridone (or cyanide), and pyrrolic functional groups similar to PANC and an additional peak at ^-405 eV, which is consistent with the presence of pyridine *N*-oxide surface species. PANCN673 showed that only pyridinic, pyridone (or cyanide), and pyrrolic functional groups were present, and the spectrum was very similar to that of PANC. The pyridine *N*-oxide functional groups decompose with heat treatment < 673 K (see Figure 1).

High-Temperature Gasification Treatment Series. The XANES spectra of GNA and GNA-B56 (GNA after 56% burnoff in air) are shown in Figure 1. The absence of a peak at 405 eV in the spectrum of GNA indicates that pyridine *N*-oxide groups are not formed in high-temperature ammonia treatment. This is consistent with the thermal stability shown by heat treating carbon GN in an inert atmosphere. The XANES spectra of GNA and GNA-B56 are quite similar except for a small increase in the peak at ^-401 eV in the latter which is assigned to the pyridone functionality produced during combustion.[14] The XANES spectra of GA, GNA, and GNA-B56 are similar to oxidized PAN carbons in the region up to 404 eV except that the relative intensities of the 401 and 402.5 eV peaks are lower relative to the peak at 399.8 eV due to pyridinic groups. Ammonia treatment incorporates the same functional groups as those produced by direct carbonization, but the relative concentrations are different.

Acridine Reference Carbon. The XANES spectrum of AD1073 contains a sharp peak at ^-399.8 eV corresponding to the pyridinic functionality. There is a broad, weak absorption at ^-403.5 eV and sharp peaks due to pyrrolic and pyridone (or cyano) functionalities observed for other carbons are absent. This is the simplest spectrum and is consistent with the pyridinic functional groups present in the acridine precursor.

3.1.4. XPS. Figure 2 shows the distribution of the nitrogen functional group compositions of the carbon TPD residues. The corresponding spectra are given in Supporting Information. The samples with higher nitrogen contents contain mainly quaternary nitrogen. The samples with low nitrogen contents contain larger amounts of the oxidized form at the expense of quaternary nitrogen. This may be due to surface oxidation.

3.1.5. XRD Measurements. The crystallinity of TPD carbon residues was examined by the XRD methods described previously.[39] The 002 reflection profiles were

very symmetrical, and the results calculated by the two methods were similar as shown in Table 4. AD1073R is different from the other carbons having a larger crystallite stack height *(L_c)* value which is indicative of a higher degree of stacking in the microdomains in the carbon structure. Typical values of L_c and the peak centroid ($°2\theta$) for cokes heat treated to 1673 K are L_c (27–32 Å), full width at half-maximum ($°2\theta$) ^- 2.96–3.56, and centroid ($°2\theta$) ^- 29.4–29.6°. AD1073R has similar structural crystallinity to graphitizable cokes, whereas the other carbons have lower crystallinity. This is related to the acridine precursor because the PAN carbons also have high nitrogen contents. Previous studies have shown that acridine carbon is optically anisotropic with mainly flow- and domain-type textures.[40] This indicates that the carbon has passed through a nematic discotic liquid crystal phase and, hence, is a graphitizable carbon. This is consistent with the higher crystallite stack height *(L_c)* values. The other carbons have isotropic optical texture and are nongraphitizable carbons.

3.2. TPD and TPR. The integrated concentration ratios for all the TPD and TPR measurements for CO, CO_2, N_2, NH_3, H_2, HCN, CH_4, H_2O, and NO are given in Supporting Information. The concentration data include CO_{2A} < 675 K and CO_{2B} > 675 K; CO_{2A} < 1250 K and CO_B > 1250 K; N_{2A} < 1150 K and N_{2B} > 1150 K; H_{2A} < 1350 K, H_{2B} > 1350 K, and H_{2C} consumed in TPR, corresponding to the regions of the main desorption peaks. The CO_2/CO TPD ratios for the carbons used in study ranged from 0.02 to 0.79.

3.2.1. GN and GN673 Carbons. The TPD and TPR profiles for GN and GN673 are shown in Figure 3. The TPD nitrogen species of GN are evolved over three temperature ranges, 400–800 K, 800–1200 K, and >1200 K. In the low-temperature region, 400–800 K, the NO peak was bimodal, and N_2, CO_2, and a small amount of HCN were evolved over a similar temperature range to the higher NO peak. A very small amount of NO was evolved as a very broad peak in the intermediate temperature range (800–1200 K) where CO was the main species evolved. The majority of the nitrogen species were evolved at high temperature (>1200 K). The N_2 peaked at ^-1510 K and was evolved concurrently with H_2.

During TPR of GN, the low-temperature NO and N_2 peaks increased compared with the corresponding TPD peaks. NH_3, HCN, NO, and N_2 were evolved in the intermediate temperature range where hydrogen consumption reaches a maximum at ^-1000 K. In the highest temperature range, the N_2 evolution decreased markedly. The peak in hydrogen consumption was almost coincident with the NH_3, HCN, NO, N_2, CO, and CO_2 peaks. Significant methane production through carbon gasification was not observed. These observations are evidence for hydrogen chemisorption capping active sites, as well as gas-phase reaction of radicals/species. The N_2 TPR profile also had peaks at 1035, 1160, and 1440 K whereas

(39) Feret, F. R. *Analyst* **1998,** *123,* 595.
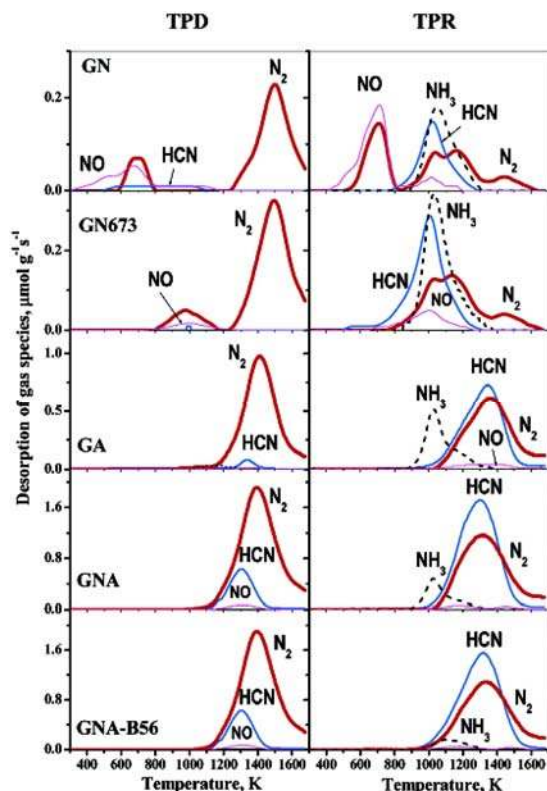
(40) Wang, W.; Thomas, K. M. *Fuel* **1992,** *71,* 873.

Figure 3. TPD profiles for G carbons.

Figure 4. TPD profiles for PANC and acridine carbons.

the TPD profile had one main peak at ^-1510 K over the temperature range. The hydrogen atmosphere perturbs nitrogen surface group reactions increasing HCN and NH₃, while decreasing N₂ formation.

3.2.2. GA, GNA, and GNA-B56 Carbons. The TPD/TPR profiles for GA and GNA are shown in Figure 3. Ammonia treatment at 1073 Kinvolves reactions ofN or NH radicals with graphene layers and nitrogen incorporation is larger after oxidation pretreatment (see Table 2). The nitrogen species desorb during TPD mainly as N₂ (above ^-1200 K) and smaller amounts of HCN and NO. The TPD HCN/N₂ concentration ratio for GNA is higher than for GA while the corresponding ratios are similar under TPR conditions. The other difference is the appearance of significant NH₃ peaks and reduction in N₂ under TPR conditions. These trends are also observed for GNA-B56 but show only minor differences in the profiles compared with those of GNA.

3.2.3. PANC and PANCN Series of Carbons. The TPD profiles of PANC and PANCN are compared in Figure 4. TPD peaks were observed for PANCN centered for NO at ^-550 K and N₂ at ^-600 K, which were not observed for the PANC. Similar NO and N₂ peaks due to the decomposition of pyridine *N*-oxide groups were observed in the TPD profiles of GN as shown in Figure 3. Very little HCN was evolved over this temperature range. However, there were some differences between the low-temperature NO and N₂ TPD profiles of GN and PANCN. In the case of the TPD of GN, the NO peak was bimodal with peaks at 520 and 660 K while the N₂ peak was narrower reaching a maximum at 695 K with no evidence of a low-temperature component. The corresponding NO TPD peak for PANCN is broad and not resolved into components. The low-temperature NO and N₂ TPD peaks are progressively removed by heat treatment (see Figure 5). This coincides with the loss of the 405 eV XANES peak, assigned to pyridine *N*-oxide functional groups (see Figure 1). These NO and N₂ peaks coincided with peaks for the evolution
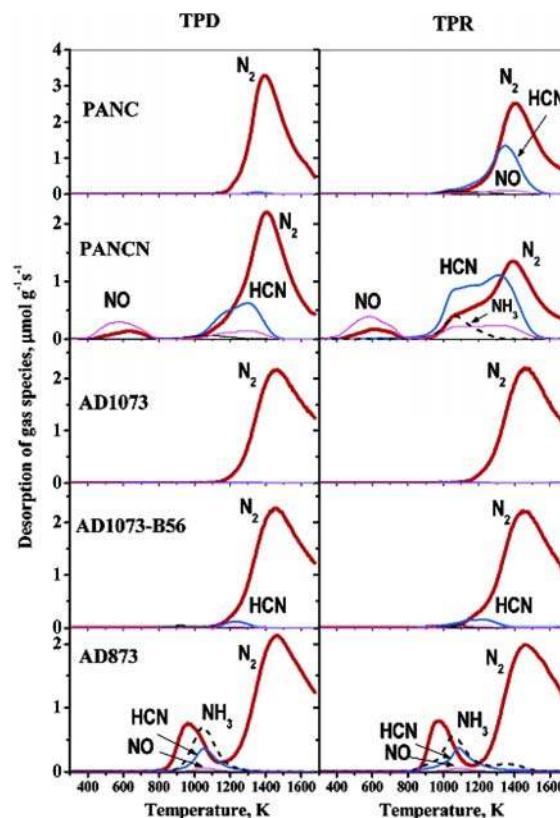
ofCO₂ at ^575 K due to decomposition ofcarboxylic surface groups. The CO₂ TPD profiles for both GN and PANCN carbons have similar shapes.

The TPD profiles for nitrogen-containing species of PANC start at ^-1200 Kwith HCN and NO peaks at ^-1350 K and N₂ at 1390 K. The NO and larger HCN TPD profiles for PANCN are broader than for PANC carbon, and both peaks occur at ^-1230 K. A small NH₃ peak is observed at ⁻1090 Kin the TPD of PANCN. These peaks due to release of nitrogen-containing species are well above the corresponding CO profile peak at ^-980 K. The N₂ profile peak occurred at 1410 K while the H₂ profile was at ^-1300 K. The CO evolved in this temperature range was relatively small compared with the lower temperature part of the TPD profile.

TPD profiles for N₂, from the PAN series of carbons, peak at ^-1400 Kand decrease to <20% oftheir maximum value by 1673 K, the limit of the instrument. The majority of the nitrogen in the carbons was desorbed as N₂ while the rest was evolved as HCN, NH₃, and NO. Approximately 80% of the desorbed nitrogen species was evolved above ~1200 K. NO was <5% and mainly desorbed over the range 500–700 K. This NO is due to decomposition of pyridine *N*-oxide groups. Chemical analyses of the TPD residues (see Table 2) show that that all the samples contained ^-2.2–2.4 wt % daf of nitrogen but very little oxygen. This indicates that ^- 28% ofthe original nitrogen was retained in the TPD residue. In excess of 95% of the total CO₂ was desorbed by 873 K. The oxygen contents of the carbons did not have an effect on desorption of N₂. This is due to the limited overlap of the decomposition ranges of the functional groups.

The TPR profiles of PANC and PANCN are shown in Figures 4 and 5. The HCN peak for the TPD PANC, which showed evidence for two components, became clearly bimodal under TPR conditions with the lower peak shifting
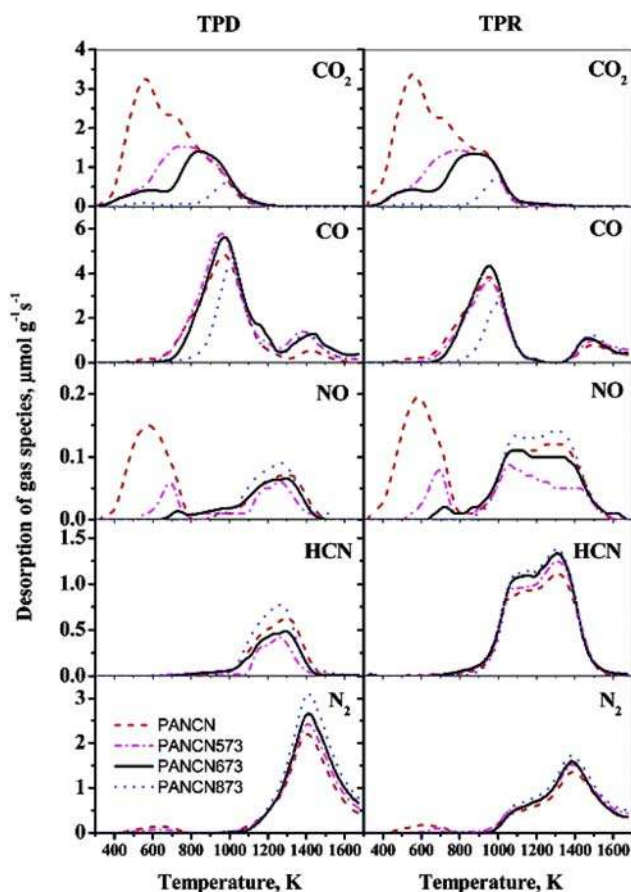
Figure 5. TPD and TPR profiles for the PANCN carbon series.

Figure 6. Comparison between TPD (0) and TPR (9) data and analytical data for oxygen; solid line is $y = x$.

Figure 7. Comparison between TPD (O) and TPR (0) data, mass balance (TPD + TPD residue (b), and analytical data for nitrogen: solid line is $y = x$.

to 1100 K with the other peak at 1320 K, which is higher than the corresponding TPD peak at 1275 K. The nitrogen peak also became bimodal with a peak at ^-1100 K and a much larger peak observed at 1400 K. The latter temperature is similar to the TPD peak observed for N_2. Therefore, the presence of hydrogen enhanced the formation of HCN, NH_3, and N_2 at ^-1100 K but reduced N_2 evolution at 1400 K.

Comparison of the TPD and TPR integrated concentration data for the G, PANC, and ammonia treated series of carbons show that the major differences are the increase in HCN and NH_3 and reduction in N_2 concentration under reducing conditions. This clearly indicates the role of surface H species in forming HCN and NH_3. Surface oxygen species (O/C range 0–0.2) do not have a significant influence on char nitrogen conversion to NO under the conditions used in this study.

3.2.4. Acridine Derived Carbons. The TPD and TPR profiles of the AD series are shown in Figure 4. N_2 is the main TPD product, and the profile peaks at ^-1500 K and extends above the maximum temperature (1673 K) ofthe instrument. Analysis ofthe TPD residue shows that ^-40% of the original nitrogen was retained in the char at 1673 K. XPS studies show that this stable functionality is mainly quaternary nitrogen (see Figure 2).[12] Abroad, weak HCN TPD peak was observed at 1285 K while the hydrogen peak was at 1270 K. The TPD profile of AD1073-B56, which has been subjected to partial combustion, displays a small HCN peak. [14] Previous XANES studies have shown that partial combustion samples contain pyridone, carboxylic anhydride, and carbonyl groups.[14,41] AD1073

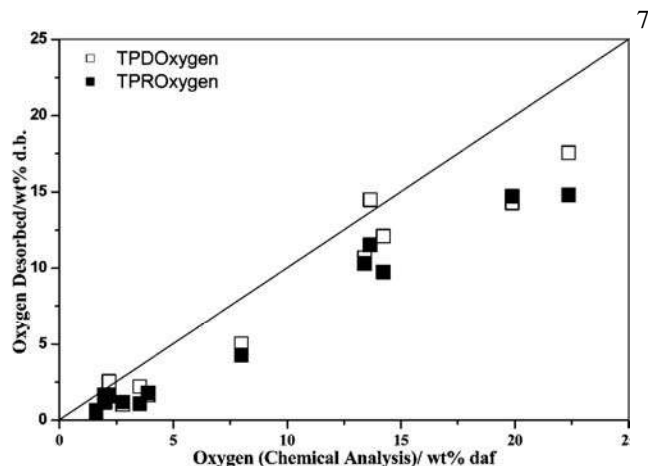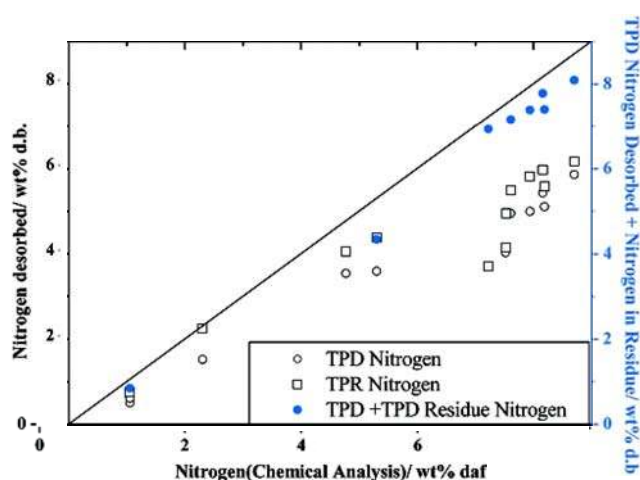(41) Turner, J. A.; Thomas, K. M. *Langmuir* **1999**, *15*, 6416.

desorbs the largest amount of H_2 during pyrolysis in the temperature range 800–1350 K due to the growth of graphene layers in the graphitizable carbon (see Supporting Information) so that TPR has little effect on the evolution of nitrogen-containing species.

3.2.5. Integrated Concentrations of TPD and TPR Species. Figure 6 shows graphs of the amount of oxygen desorbed during TPD and TPR against oxygen content of the carbon. Both graphs are linear, and the lines pass through the origin within experimental error (TPD gradient 0.828 (0.055 and intercept –0.44 (0.61; TPR gradient 0.746 (0.037 and intercept 0.41 (0.42). Chemical analysis showed that the TPD residues contained < 0.2 wt % oxygen but significant amounts of nitrogen (see Table 2). The oxygen mass balance difference is attributed to physisorption of oxygen-containing species, which are not detected by mass spectrometry sampling. Nitrogen-containing products do not suffer from this problem. Figure 7 shows that graphs of nitrogen desorbed in the TPD and TPR experiments versus nitrogen content of the carbon are approximately linear and pass through the origin within experimental error (TPD gradient 0.630 (0.043 and intercept 0.01 (0.28; TPR gradient 0.631 (0.064 and intercept 0.41 (0.42). The total nitrogen in the species detected by TPD is lower than that obtained from the corresponding chemical analysis. Figure 7 also shows a graph of the sum of nitrogen desorbed during

TPD and nitrogen retained in the TPD carbon residue versus nitrogen in the original carbon. A linear relationship passing through the origin within experimental error (gradient) 0.968 (0.039; intercept 0.31 (0.28; R) 0.995) is observed. The good mass balance indicates that all the major nitrogen species and desorption surface reactions were taken into account in the TPD experiments.

3.2.6. Reaction and Desorption ofSurface Species under Inert and Hydrogen Atmospheres. The TPD profiles of oxygen surface groups overlap, and peak deconvolution has been widely used to establish the chemical nature of the different surface oxygen species in carbons. Prior assumptions on the mechanism of desorption and on the distribution of the sites are often made.[34] The problems that have been encountered are as follows:

(i) Some peaks or shoulders in the CO and CO_2 profiles can be due to the same functionality, but with different desorption energy, and not necessarily due to different functionalities.

(ii) Many desorption processes, in particular those taking place inside pores, occur with readsorption.

(iii) Surface reactions may occur giving rise to evolution of products.

(iv) Assumptions include the presence of a continuous Gaussian distribution of desorption energies and that the preexponential factor is equal for all states.[34]

Therefore, TPD profiles can be used to establish the total amounts of CO and CO_2 evolved quantitatively and to identify functional groups in a semiquantitative manner. The stability of oxygen acidic functional groups is generally accepted to be

pyrone/chromene >
    phenolic/semiquinone/carbonyl   >
        lactone/lactol > –COOH

In TPR, hydrogen may (a) react with the carbon active sites formed by desorption of surface complexes, (b) reduce surface complexes, and (c) induce secondary reactions. Previous comparisons of TPR and TPD for thermal desorption of CO, CO_2, and water vapor have shown that hydrogen may (a) make the desorption of carboxylic anhydride more facile, (b) some CO surface groups (probably semi-quinone) can be directly reduced by hydrogen to give water, and (c) net hydrogen evolution from the carbon surface starts at temperatures above 1150 K. Hydrogen does not appear to directly reduce carboxylic acid anhydride groups, which desorb as CO and CO_2 in a ^-1:1 stoichiometric ratio at ^-900 K.[42,43] However, it chemisorbs on sites created by desorption of the species and reduces oxygen surface species at high temperature.

The TPR peaks are shifted to slightly lower temperature compared with TPD, and in the case of carbons with high concentrations of oxygen functional groups, it makes the peaks multimodal. There is little change in the profiles of CO and CO_2 below ^-750 K. The amounts of CO evolved for TPR are lower than the corresponding values for TPD while the corresponding amounts of H_2O are higher for TPR than for TPD.

The presence of a hydrogen atmosphere, compared with an inert atmosphere, shifts the NH_3 and HCN peaks to lower temperature and increases the amounts of HCN and NH_3 evolved with a corresponding decrease in N_2. The stoichiometry of hydrogen consumed in relation to the nitrogen species desorbed is difficult to calculate because ofthe dominance ofthe CO species. NH_3 is evolved

in the range where hydrogen is desorbed, whereas the oxygen functional groups are desorbed at lower temperature. Comparison of TPD and TPR shows that changes in surface oxygen groups have limited influence on reactions of nitrogen species.

3.3. Thermal Stability of Surface Nitrogen Species.
Nitrogen retention during TPD is smaller for GNA (14%) than for either the PAN series of carbons (^ 28%) or AD1073 (42%) and is independent of the oxygen content for the PAN series. Heat treatment leads to growth of graphene layers and formation of more stable quaternary nitrogen located in the interior ofthe graphene layers.[12,36,44] Quaternary nitrogen formation occurs above the ammonia treatment temperature and, therefore, is smaller for GNA. The highest nitrogen retention was observed for the acridine char, which is a graphitizable carbon.

Nitrogen functionalities such as pyridones, protonated pyridinic *-N* and pyridinic *N*-oxides are converted to pyridinic *-N* under mild pyrolysis conditions, and pyrrolic-*N*is converted to pyridinic-*N*during carbon structural development. [12-15,44] Pyrolysis to higher temperatures results in formation of pyridinic-*N* located at the edge of the graphene layers or quaternary-*N* in the interior ofthe graphene layers.[12,43-47] The order of thermal stability of nitrogen functional groups is as follows:

$$\text{–C}(N\text{-quaternary}) > \text{–C}(N\text{-pyridinic}) > \text{–C}(NH \text{ pyrrolic}) > \text{–C}(NO)$$

The nitrogen functional group composition of acridine carbons did not vary markedly for HTTs in the range 873-1273 K.[12] Acridine carbon AD1073 contained pyridinic ^-20%, quaternary – 61%, and N–X – 19%,[12] while the composition ofthe TPD residue (AD1073R) was pyridinic ^- 5%, quaternary – 84%, and N–X – 11%. TPD studies showed that only – 58% of the nitrogen in AD1073 was desorbed during TPD to 1673 K. PANC carbon with a pyrolysis temperature of 1073 K had the composition pyridinic ^- 40%, pyrrolic ^- 29%, quaternary – 23%, and N–X – 9%. These results are consistent with the differences observed in the XANES spectra where bands observed at ^-401 and 402.6 eV are due to pyridone and pyrrolic functional groups. The composition ofthe nitrogen functional groups in the TPD residue, PANCR, was pyridinic ^- 18%, quaternary – 67%, and N–X – 15%. Comparison of the integrated intensity data for TPD profiles of nitrogen species (see Supporting Information) and analytical data (Table 2) shows that < 10% is desorbed below ^-1200 K, the major portion is desorbed as N_2, and some is retained in the char (HTT 1673 K). N_2 results from reaction of surface species rather than the direct decomposition product of a surface group. Therefore, direct desorption of nitrogen functional group species is not the major mechanism and quantification of the nitrogen functional groups from TPD profiles is not appropriate.

The conversion of quaternary nitrogen to NOx under combustion conditions is a major issue. XANES showed that pyridone, carboxylic anhydride, and carbonyl groups were formed during the carbon combustion. [14,41] These groups appear to have little effect on desorption ofnitrogen species from AD1073-B56 and GNA-B56. Kapteijn et al.[48] investigated the gasification ofnitrogen-containing model

(42) Calo, J. M.; Cazorla-Amoros, D.; Linares-Solano, A.; Roman-Martinez, M. C.; Salinas-Martinez de Lecea, C. *Carbon* **1997**, *35*, 543.
(43) Otake, Y.; Jenkins, R. G. *Carbon* **1993**, *31*, 109.
(45) Lahaye, J.; Nanse, G.; Bagrreev, A.; Strelko, V. *Carbon* **1999**, *37*, 585.
(46) Stanczyk, K.; Boudou, J. P. *Fuel* **1994**, *73*, 940.
(47) Schmiers, H.; Friebel, J.; Streubel, P.; Hesse, R.; Ko¨psel, R. *Carbon* **1999**, *37*, 1965.
(48) Laszlo, K.; Tombacz, E.; Josepovits, K. *Carbon* **2001**, *39*, 1217.
(49) Kapteijn, F.; Moulijn, J. A.; Matzner, S.; Boehm, H. P. *Carbon* **1999**, *37*, 1143.

chars where quaternary nitrogen was the major constituent, in CO_2 and O_2. During CO_2 gasification, a slight decrease of quaternary nitrogen relative to pyridinic and pyridonic nitrogen was observed, with all nitrogen forms decreasing in absolute terms with increasing burnoff. During combustion, the absolute quantities of N-5 and N-6 remain fairly constant, while N-Q decreases. At high burnoff levels the major functionality was pyridone in O_2, while in CO_2 both pyridone and pyridinic groups were present in similar amounts. Combustion and CO_2 gasification gave differences in the development of the nitrogen functionality with burnoff.

The thermal stability of nitrogen surface groups needs to be considered in relation to the stability of –C(H) and various types of –C(O) surface groups because surface reactions occur. The pyridine *N*-oxide groups decompose in the temperature range 500–700 K to give NO and N_2 and a very small amount of HCN. Studies of the C–NO reaction using the transient kinetic approach with $_{14}N_{16}O$ and $^{15}N^{18}O$ have shown that –C(N) reacts with NO to yield N_2.[22] Previous studies[26] have shown that NO can react with char to produce –CN surface groups. The mechanism is consistent with desorption of NO and the reaction of mobile surface species –C(NO) to form N_2 as follows.

$$C(NO) + -C(NO) \ ^f N_2 + 2-C(O)$$
$$and/or \ -C(N) + -C(NO) \ ^f N_2 + -C(O)$$
$$+ -C_{fas}$$
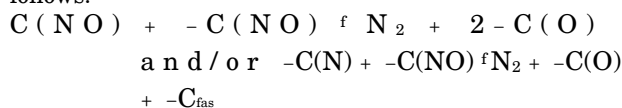
where –C(N) and –C(O) are surface species and $-C_{fas}$ is a carbon free active site. Desorption of other nitrogen surface groups from PANCN involves a small peak due to NH_3 at ^-1100 K. This is similar to the temperature (-1140 K) where the H_2O TPD profile reaches a maximum but well below the lowest temperature peak (1300 K) due to hydrogen evolution. The corresponding HCN TPD peak occurs at ^-1300 K but shows evidence for a component at lower temperature. The formation of a small amount of NO, which peaks at ^-1270 K, is in the region where the CO and H_2O peaks are decreasing and those of H_2 and HCN are increasing. The NO peak is weak but quite distinct from the NH_3 peak. NH_3 is derived from either the decomposition on pyrrolic surface groups or reactions to form NH surface species involving –C(H) species. The hydrogen desorbed is small in the temperature range of the NH_3 peak. N_2 is the major desorption product and is a product of reactions of –C(N) mobile surface groups rather than direct desorption of decomposition products of surface groups. The surface groups may also react with C(H) surface species, which are increased under TPR conditions leading to higher evolution of HCN and NH_3 with decreasing N_2 evolution. These observations are indicative hydrogenation of –NH and –C(N) surface species. The fact that the change in HCN is much greater than NH_3 suggests that surface groups –N and N–H are in lower concentration than –C(N). This assumes that C(N) does not react to an appreciable extent with –C(H) to form N(H). Therefore, HCN is formed by either the surface reaction

$$-C(H) + -C(N) \ ^f HCN + -C_{fas}$$
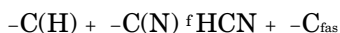
where $-C_{fas}$ is a free active site or desorption of HCN fragments from decomposition of functional groups in the carbon structure. Studies of the pyrolysis of pyridine in

quently decomposes to HCN.[49] The mechanism for decomposition of pyridinic functional groups in carbons may be similar. There is little overall loss of nitrogen species (excluding pyridine *N*-oxide groups) until this temperature range as shown by TPD and chemical analysis results. XPS studies have shown that the conversion of pyrrolic groups to pyridinic groups occurs with increasing HTT showing that pyrrolic groups are less stable than pyridinic groups. [12-14] N_2 formation occurs at high temperature where oxygen surface groups are negligible mainly, via the surface reaction

$$-C(N) + -C(N) \ ^f N_2 + -2C_{fas}$$

where $-C_{fas}$ is a free active site and one of the surface species must be mobile. Evidence for the presence of mobile –C(N) surface groups also comes from the observation of C_2N_2 and HCN in temperature programmed combustion and HCN in TPD.[27] C_2N_2 is stable at the lower temperatures in the temperature programmed combustion, but it is unstable above ^ 900 K and, therefore, is not observed in the TPD studies.

4. Conclusions

The thermal evolution, stability, and reactivity of nitrogen surface functional groups in four suites of carbons, with varying amounts of oxygen and nitrogen functional groups, were investigated by TPD and TPR. The functional groups were characterized by XANES and XPS. The TPD and TPR results are quantitative and show that the oxygen and nitrogen groups have markedly different thermal stabilities and reactivities. The decomposition temperature ranges of surface groups and the reactions of mobile surface species control the desorption products. Specific nitrogen functional groups decompose over temperature ranges to give mobile species, which may either desorb, react to form products which are desorbed, or be incorporated in the graphene layer structure. Pyridine *N*-oxide surface groups desorb NO and form N_2 via surface reactions. Pyrrolic functional groups are preferentially converted to pyridinic and quaternary nitrogen species in the carbon structure during heat treatment. The high thermal stability of pyridinic and quaternary nitrogen surface species mainly results in mobile species at high temperatures and concurrent desorption of nitrogen-containing species with hydrogen. A major part of the oxygen surface species were desorbed at lower temperatures than those at which the nitrogen species become mobile and have little or no effect on the conversion of char nitrogen to NO under TPD conditions. In comparison, under TPR conditions, the hydrogen atmosphere shifts the peaks to slightly lower temperature and in those cases where there are oxygen functional groups in large amounts it makes the peaks multimodal. This suggests that the oxygen has a role in the region where H_2 is consumed and H_2O, NH_3, and HCN are formed. Decomposition of nitrogen surface groups at low temperature primarily leads to retention of nitrogen in the carbon structure rather than desorption of nitrogen-containing gaseous species. Significant amounts of nitrogen species are not desorbed until > 1200 K, and even after heat treatment to 1673 K, —15-40% of the original nitrogen is retained in the carbon structure as quaternary nitrogen. This is probably related to carbon structural development and contrasts with oxygen surface species which are desorbed at lower

(49) Ikeda, E.; Mackie, J. C. *J. Anal. Appl. Pyrolysis* **1995**, *34*, 47.

temperatures. The assignment of TPD peaks to specific functional groups is not appropriate when the main reaction pathways are reaction of surface species to give gaseous products and incorporation of nitrogen in the carbon structure rather than direct desorption of decomposition products of surface species.